

Plasma modelling by commercially available fluid flow and electromagnetic simulators for plasma processing

I. Ganachev^{1,2}, S. Kono¹, S. Nakao¹, Y. Toyota², H. Sugai¹

¹ Nagoya University, Nagoya, Japan

² Shibaura Mechatronics Corporation, Yokohama, Japan

1. Introduction

Plasma modelling and numerical simulations are usually performed by non-commercial software codes. Such approach is unavoidable when applying new modelling/simulation techniques. Some codes, in particular PCC-MCC (Particle-in-Cell Monte-Carlo Collisions) one and two-dimensional codes are also available for free downloads [1]. Reaching steady state in PCC-MCC simulation requires still too long computational times on today's commonly available desk-top workstations, and is therefore not suitable for wide use in the design of plasma processing installations, thus less time-consuming fluid and hybrid codes are necessary. However, the demand for plasma simulation is still limited, resulting in a small niche market not large enough to attract simulation software vendors. As a result there are very few commercial simulation packages capable of self-consistent plasma simulation. Packages developed by major universities rely on the support of major manufacturers of plasma processing equipment and are therefore kept in-house and treated as important intellectual-property secrets.

On the other hand, the huge market for electromagnetic and fluid flow simulators resulted

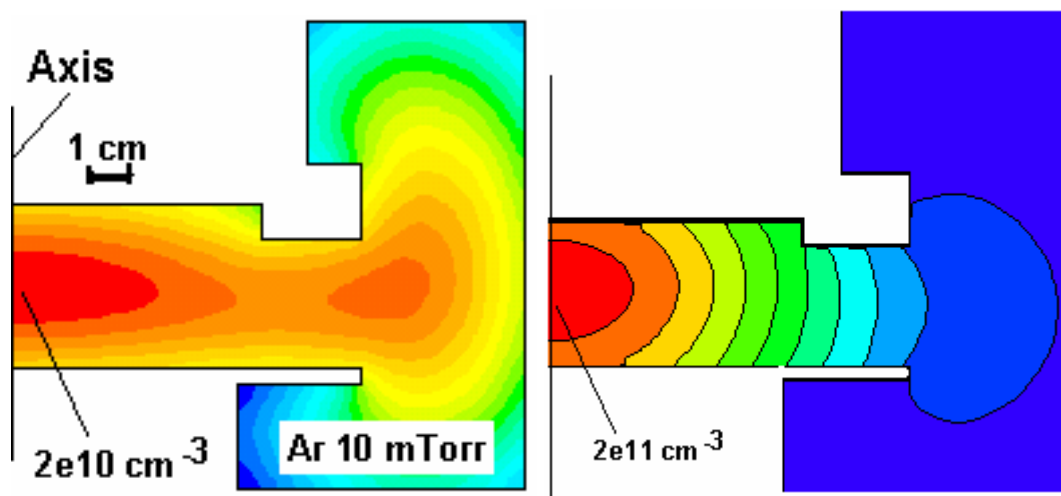


Fig. 1. Plasma density profile in a GEC ICP cell at 150 W. Left: assuming uniform electron temperature; right: assuming bulk electron temperature 2eV higher than near the walls.

in a wide selection of competing simulation codes offered in various price ranges and featuring reasonable computation times. In the present contribution we show how a combination of such codes can be used for simulation of low-temperature argon ICP and microwave plasmas at medium gas pressures (tens of mTorr).

2. Fluid flow simulations for capacitively coupled plasma

The basic equations to be included in any more or less realistic plasma model of a low-temperature ambipolar-diffusion controlled argon plasma must be:

Quasi-neutrality (postulates that ions and electrons should diffuse together)

$$n_e = n_i = n \quad (1)$$

Particle balance equation in the plasma volume (ionization should compensate the diffusion loss locally)

$$\nabla \cdot D_a(T_e) \nabla n + \nu_i(T_e) n = 0 \quad (2)$$

Bohm criterion at the plasma boundary (determines the rate of charged particle loss via wall recombination, \mathbf{n} is the boundary normal unit vector)

$$D_a(T_e) \mathbf{n} \cdot \nabla n = \nu_B(T_e) n \quad (3)$$

Energy loss per ion-electron pair reached the wall as function of the electron temperature T_e

$$\Delta \varepsilon(T_e) = kT_e [2 + \ln(m_i / 2\pi m_e)] + E_c(T_e) \quad (4)$$

Those equations include the following quantities, all dependent on the electron temperature:

Ambipolar diffusion coefficient D_a (ion diffusion coefficient times $(1 + T_e / T_i)$).

Ionization collision frequency ν_i

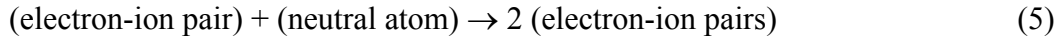
Bohm velocity at the plasma boundary ν_B (determines the rate of particle loss)

Inelastic collision loss power $E_c(T_e)$ and other losses per one ion-electron pair reaching the plasma boundary (determines the power necessary to sustain the plasma).

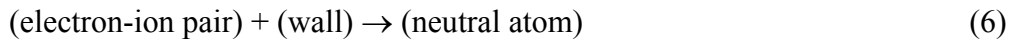
In equations (1-4) m_i and m_e are the ion and electron mass, respectively, and k is Boltzman's constant.

Such a formulation of the plasma production is treatable with most commercial fluid flow simulators. The assumption of quasi-neutrality reduces the number of different types of

species to be considered to only two: neutral argon atoms and ion-electron pairs. The particle transport is treated as diffusion of the electron-ion pairs to the walls. The ionization is treated as a volume chemical reaction



with the ionization rate determined by the local electron temperature. Volume recombination and step ionization are negligible and the particle loss is dominated by recombination at the wall. In a fluid flow simulator it can be expressed as a surface reaction



with the reaction rate equal to the Bohm velocity (again determined by the local electron temperature). The electron temperature can be computed from the plasma electron thermal conductivity and the power deposition profile (also possible in a standard fluid flow simulator), or alternatively be introduced as a known profile with known value at the chamber walls and unknown peak value T_e^{\max} somewhere in the plasma volume. In the last case T_e^{\max} can be found from the condition that the bulk ionization and surface recombination should compensate. This approach is demonstrated at the example of the ion density profile in a standard GEC ICP cell [2] shown in Fig. 1 for two assumptions – neglecting the spatial variation of the electron temperature (left figure) and with electron temperature difference of about 3 eV between the coldest area near the wall and the hottest bulk region (right figure). The second approach results in higher density in the bulk, which is consistent with measurement data indicating peak density of the order of 10^{11} cm^{-3} [3].

3. Electromagnetic field simulations for surface wave plasma

Commercial electromagnetic field simulators can be directly applied to plasmas after introducing the plasma permittivity

$$\varepsilon_p = 1 - \frac{n}{n_c} \left(1 - i \frac{V_m}{\omega} \right), \quad (7)$$

where n_c is the critical plasma density and ν_m is the electron-neutral collision frequency for momentum transfer. Thus one can obtain the RF electric field profile (related to the power deposition profile) and the plasma impedance. In Fig. 2 we demonstrate the resonant behaviour of surface-wave microwave plasma based on a two-dimensional simplified model [4]. The microwave is poorly absorbed by the plasma except for specific frequencies, where the distance between the chamber walls becomes a multiple of half the surface-wave wavelength. The model itself and one of the resonant modes are shown in Fig. 3. The importance of the plasma density is demonstrated by the difference of the absorption spectra for low and high plasma density (left and right plots in Fig. 2, respectively).

References: [1] V. Vahedi et al: *Phys. Fluids B* **5** (1993), pp. 2719-2729.
 [2] J. K. Olthoff: *J. Res. Natl. Inst. Stand. Technol.* **100** (1995) 327.
 [3] P. L. G. Ventzek et al.: *J. Vac. Sci. Technol.* **B-12** (1994) 3118.
 [4] I. Ganachev and H. Sugai, *Plasma Sources Sci. Technol.* **11** (2002) A178-A190.

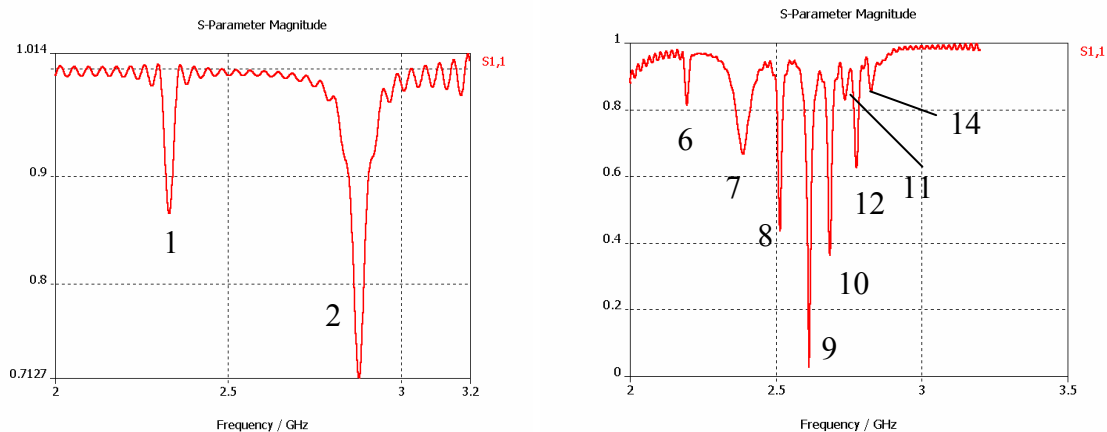


Fig. 2. Microwave absorption spectra for underdense/overdense plasma: left $n = 5.5 \times 10^{10} \text{ cm}^{-3}$ (underdense plasma), right $n = 5.5 \times 10^{11} \text{ cm}^{-3}$ (overdense plasma). The numbers under the individual resonances indicate the number of half wavelengths in the standing-wave pattern.

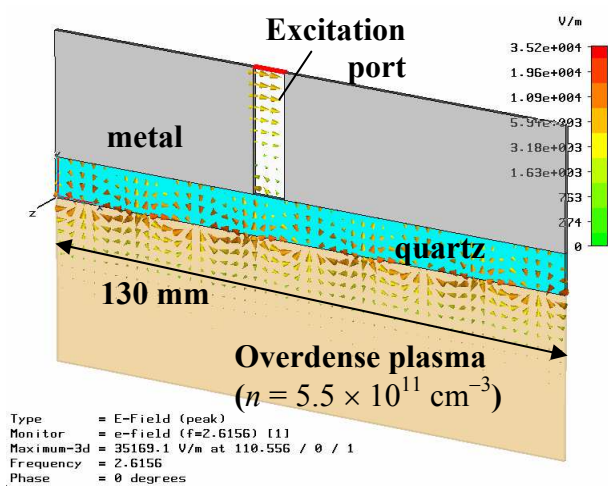


Fig. 3. Electric field configuration for the 9th mode from Fig. 2 right.